

Performance analysis of a 320-Gbps integrated MDM-DWDM-FSO transmission link under adverse weather conditions

KARAMJEET SINGH¹, MEHTAB SINGH², AMIT GROVER^{1,*}

¹Department of Electronics and Communication Engineering, Shaheed Bhagat Singh State University, Punjab, India

²Department of Electronics and Communication Engineering, University Institute of Engineering, Chandigarh University, Mohali, Punjab, India

This research work reports the modeling of an integrated mode-division-multiplexing (MDM) dense-wavelength-division-multiplexing (DWDM)-based terrestrial free-space-optics (FSO) transmission system. 16 independent laser channels ranging from 193.1 THz – 194.6 THz with a channel spacing of 100 GHz, with each wavelength channel utilizing two spatial Laguerre-Gaussian (LG) modes (LG_{0,0} and LG_{0,20}), each transporting 10-Gbps of non-return-to-zero data are multiplexed and transmitted over free-space channel under complex weather conditions. The net transmission speed of the system is 320-Gbps. Using simulative analysis, the reported FSO link is evaluated for clear, rain, haze, and fog weather conditions using signal-to-noise-ratio and eye diagrams as the metrics for performance evaluation. The reported results demonstrate reliable 320-Gbps transmission along FSO range of 780 m – 6 km with reliable performance metrics.

(Received January 7, 2024; accepted April 8, 2024)

Keywords: Dense-wavelength-division-multiplexing (DWDM), Free-space-optics (FSO), Weather attenuation, Signal-to-noise-ratio (SNR), Eye diagrams

1. Introduction

Free-Space-Optics (FSO) has emerged as a potential technology in the pursuit of high-speed and dependable communication systems, providing a feasible alternative to conventional wired communication networks. FSO utilizes modulated light beams to transmit data in free space, offering a cost-efficient and adaptable option for point-to-point communication links [1]. The integration of Mode Division Multiplexing (MDM) and Dense Wavelength Division Multiplexing (DWDM) in FSO systems has been a central focus for researchers and engineers due to the increasing demands for higher bandwidth and faster data transmission rates [2, 3].

FSO, or optical wireless communication, utilizes modulated optical signals to transmit data over the atmosphere, enabling fast data transfer without the use of physical wires. FSO systems commonly employ lasers to transfer data wirelessly, making use of the extensive bandwidth offered by the optical spectrum. This technology has become prominent in situations where it is not feasible to establish standard cable communication infrastructure, such as metropolitan regions with difficult topography or areas susceptible to natural disasters [4, 5].

FSO offers a significant benefit in its capacity to deliver fast and efficient communication with very little delay, making it well-suited for applications like connecting the final stretch of network, corporate networking, recovering from disasters, indoor communication, satellite communication, and photonic radars [6-13]. Nevertheless, FSO technology encounters

obstacles such as air absorption, scintillation, and vulnerability to weather conditions. These issues require inventive approaches to improve the dependability and efficiency of FSO [14].

DWDM is a commonly used technology in optical communication systems that aims to optimize the use of the available optical spectrum. DWDM enables the concurrent transmission of many data streams over a single optical fiber by allocating each signal to a distinct wavelength. DWDM plays a crucial role in contemporary optical networks due to its ability to significantly enhance data transfer capacity.

In the past, optical communication systems have typically increased their capacity by utilizing techniques such as WDM and DWDM. MDM, on the other hand, utilizes the spatial degrees of freedom that naturally exist in optical fibers [15, 16]. Light in an optical fiber can travel in many modes, each characterized by a distinct spatial pattern of intensity. MDM utilizes distinct modes as separate data channels, allowing for the concurrent transmission of multiple data streams across a single optical cable [17]. The introduction of MDM offers an extra layer of multiplexing, which allows for a more efficient utilization of the optical spectrum. Each individual mode present in the optical fiber functions as a separate route for data, resulting in a significant growth in transmission capacity when compared to conventional multiplexing methods. This methodology signifies a fundamental change in optical communication, providing a new method to overcome existing restrictions on data

transfer capacity and meet the increasing data requirements of contemporary applications.

MDM, when included into FSO transmission systems, offers various advantages that improve communication performance. An important benefit is the possibility of higher data transmission speeds. MDM enhances the bandwidth capacity of FSO networks by utilizing many spatial modes simultaneously [18, 19]. This technology effectively meets the increasing demand for higher data transfer rates. Moreover, MDM possesses the intrinsic capability to alleviate the influence of meteorological circumstances on signal quality. The use of many modes enables FSO systems to achieve diversity, enabling them to adjust to the ever-changing and uncertain conditions of the free-space channel [20]. The resilience of the system is especially important in situations where conventional FSO systems may encounter signal deterioration caused by causes such as scintillation, rain, or fog. H. Singh et al. in [21] reported a high-capacity hybrid MDM-passive optical network (PON)-FSO transmission along 100 – 1000 m FSO range with 10 – 20 km fiber transmission. R. Miglani et al. [22] reported a 20 Gbps MDM-PON-FSO transmission using forward error correction coding under fog weather. The performance of MDM-FSO transmission under turbulent atmosphere using multi-input multi-output has been reported by J. Zhang et al. in [23]. A spectral efficient 80 Gbps MDM-polarization division multiplexing (PDM)-multi mode fiber (MMF)-FSO transmission along

100 m MMF and 1400 m FSO has been reported by S.A. El-Mottaleb et al. in [24]. A 640 Gbps PDM-MDM-orthogonal frequency division multiplexed (OFDM)-FSO transmission along 2.2 km has been reported by D. Kakati et al. in [25].

Integrating MDM with DWDM transmission in FSO systems can improve the overall performance and scalability of the communication channel and shows significant potential in meeting the increasing need for secure, long-range, and high-capacity communication connections across several fields.

This research work investigates the synergistic relationship between FSO with MDM and DWDM technology to enhance the comprehension and advancement of high-performance, resilient, and scalable FSO communication systems by thoroughly examining effect of adverse weather conditions. The main novelty of this work is to enhance the spectral bandwidth efficiency, scalability and data rate of the optical wireless communication link by incorporating DWDM technique and MDM technique to attain > 100 Gbps data rates.

2. System design

Fig. 1 elucidates the system design of the proposed integrated MDM-DWDM-FSO transmission link.

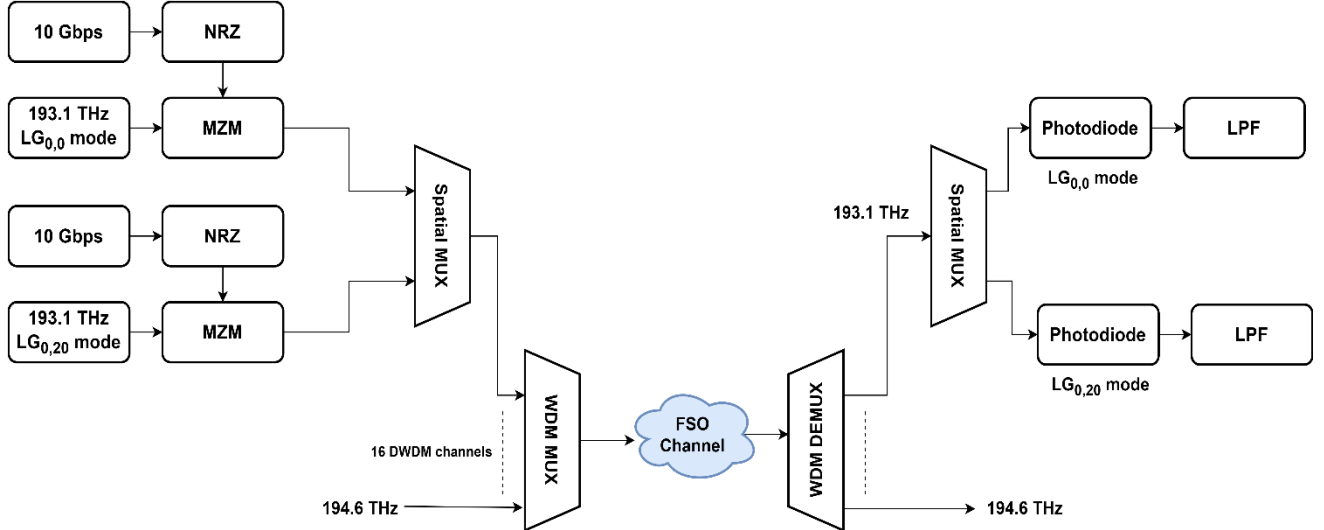


Fig. 1. Integrated MDM-DWDM-FSO transmission link

In the proposed study, we have integrated 16-DWDM channels, ranging from 193.1 THz – 194.6 THz with a channel spacing of 100 GHz. Each wavelength channels utilizes 2 MDM-Laguerre-Gaussian (LG) modes i.e., $LG_{0,0}$ and $LG_{0,20}$. Each LG mode transports 10 Gbps of non-return-to-zero (NRZ) data. The net transmission speed of the system is $16\lambda \times 2$ spatial modes \times 10 Gbps = 320 Gbps.

At the transmitter section, the 10 Gbps input data is NRZ encoded and modulated over distinct LG mode of 193.1 THz laser. The LG mode can mathematically be modelled as [26]:

$$\psi_{m,n}(r, \varphi) = \left(\frac{2r^2}{w_0^2}\right)^{\frac{|n|}{2}} L_m^n \left(\frac{2r^2}{w_0^2}\right) \exp\left(\frac{r^2}{w_0^2}\right) \exp\left(j\frac{\pi r^2}{\lambda R_0}\right) \begin{cases} \sin(|n\varphi|), & n \geq 0 \\ \cos(|n\varphi|), & n < 0 \end{cases} \quad (1)$$

where, m and n are representing azimuthal index and radial index respectively, R is representing the curvature radius, w_0 is representing the size of the spot, $L_{m,n}$ is representing the Laguerre-Gaussian polynomial. 2- optically modulated LG beams i.e., $LG_{0,0}$ and $LG_{0,20}$ are multiplexed using a spatial multiplexer In this work, a continuous wave laser at 193.1 THz central frequency

followed by a multimode generator component in Optisystem software is used to generate different spatial

modes. Fig. 2 represents the spatial profile of LG modes and summed modes.

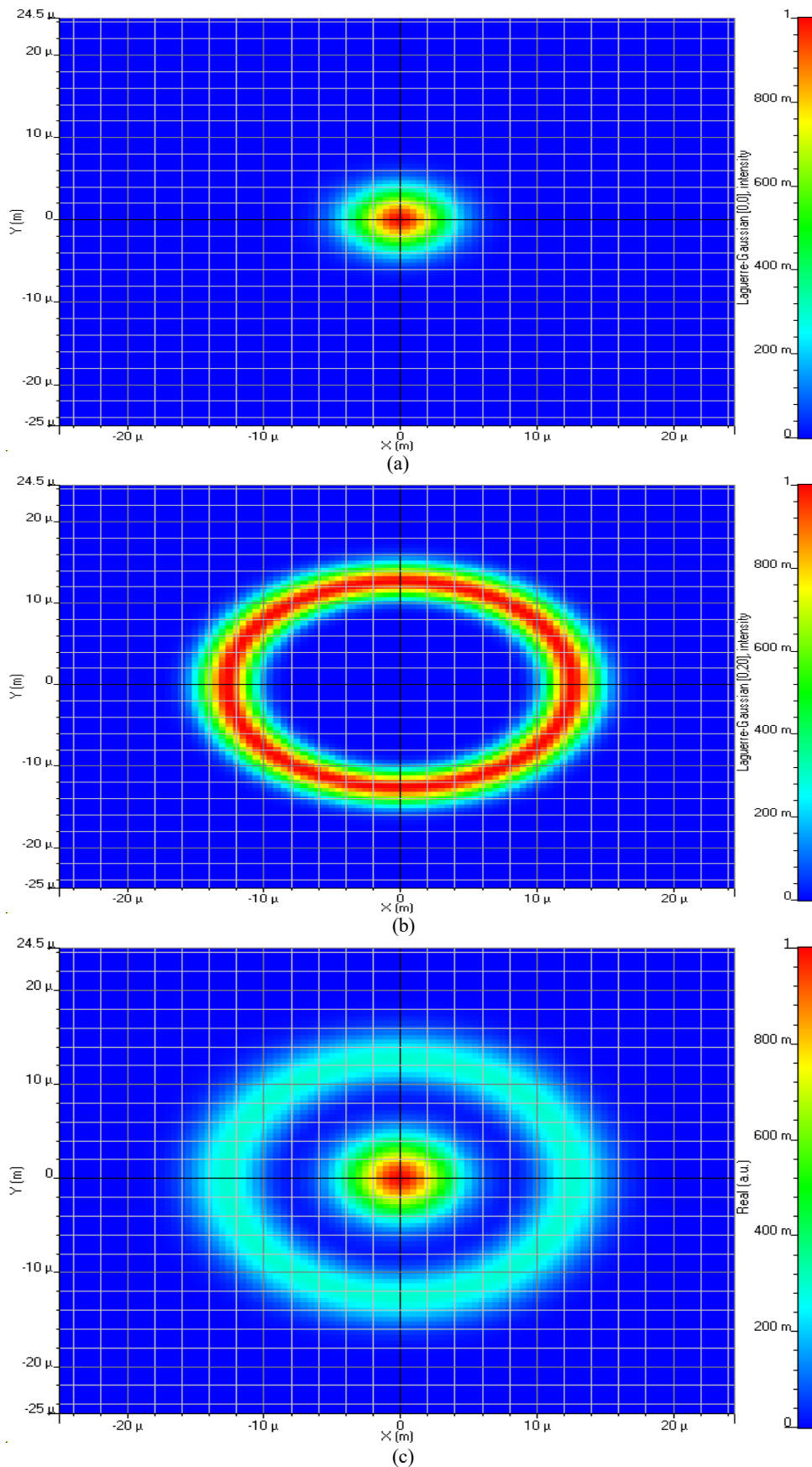


Fig. 2. (a) $LG_{0,0}$ mode (b) $LG_{0,20}$ mode (c) Summed mode (color online)

Spatial modes of all the 16-wavelength channels ranging from 193.1 THz – 194.6 THz are combined using WDM multiplexer. The net 320-Gbps information signal is transmitted through the free space channel. The information-bearing laser beam experiences attenuation due to different weather conditions. The received optical power can be modelled using the following equation [27]:

$$S_R = S_T \left(\frac{d_r^2}{(d_t + \theta Z)^2} \right) 10^{-\sigma Z/10} \quad (2)$$

where, S_R and S_T are representing optical power received and transmitted respectively, d_r and d_t are representing diameter of the receiver antenna and transmitter antenna respectively, Z is the FSO range, θ is representing the beam divergence and σ is representing attenuation coefficient. Table 1 discusses the simulation parameters considered in this work.

Table 1. Simulation parameters [28, 29]

Parameters	Value
Laser frequency band	193.1 – 194.6 THz
Channel spacing	100 GHz
Power of each laser	10 dBm
Linewidth	10 MHz
Extinction ratio	10 dB
Bitrate per channel	10 Gbps
d_r	5 cm
d_t	20 cm
θ	0.25 mrad
Thermal power density of photodiode	100e-024 W/Hz
Responsivity	0.7 A/W
Attenuation coefficient	0.14 dB/km

At the receiver section, the 320-Gbps optical signal is demultiplexed into 16-independent wavelength using a WDM demultiplexer. Further, each DWDM channel is spatial demultiplexed using MDM demultiplexer. The individual 10-Gbps optical channel is first converted to electrical signal using PIN photodiode and a low pass filter (LPF) removes the noise frequency. Table 2 discusses the attenuation coefficient for different weather conditions considered in this work. The optical spectrum of transmitted signal and received signal are elucidates in Fig. 3 (a) and (b) respectively. We can see that the power in received spectrum is less than that in the transmitted spectrum. This is because as the link range increases, the signal power degradation due to attenuation increases, which results in loss of signal power at the receiver.

Table 2. Weather attenuation coefficient [28, 29]

	Attenuation in dB/km		
	Light	Medium	Heavy
Haze	1.537	4.285	10.115
Rain	6.27	9.64	19.28
Fog	9	16	22

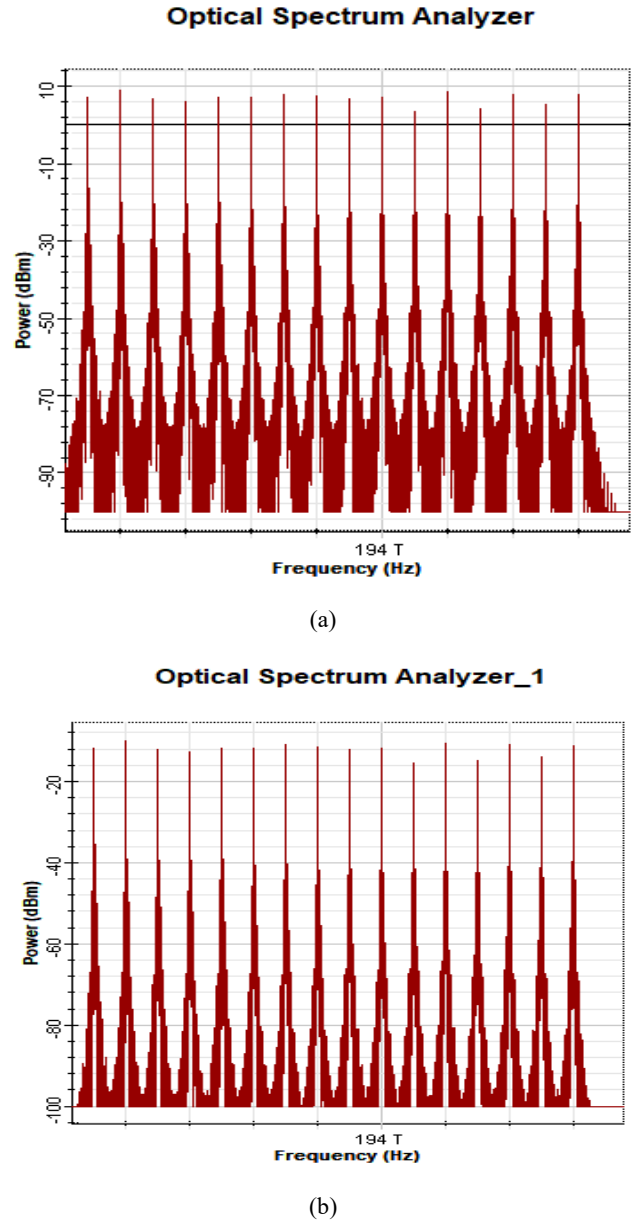


Fig. 3. Spectrum of (a) transmitted (b) received optical signals (color online)

3. Results and discussion

The proposed MDM-DWDM-FSO transmission link is investigated for complex weather conditions using signal-to-noise ratio (SNR) and eye diagrams as the metrics for performance. The results are discussed in this section.

Fig. 4 discusses the SNR plots versus increasing range for clear weather with different data rates per channel i.e., 2.5 Gbps, 5 Gbps, and 10 Gbps. Here, we have shown the graphs for channel 1 (193.1 THz- LG_{0,0} mode) only as rest of the channels show similar performance. The computed

SNR is [44.62, 32.83, 25.51] dB, [41.10, 29.30, 21.98] dB, and [38.55, 26.75, 19.43] dB at 2, 4, and 6 km FSO range respectively for 2.5 Gbps, 5 Gbps, and 10 Gbps data rate per channel. Here, we can clearly see that with increasing FSO range and data transmission rate, the SNR of the received signal degrades. The results demonstrate reliable transmission at under clear weather at 6 km range for 10 Gbps data rate per channel with acceptable SNR (~ 20 dB). Fig. 5 elucidates the eye diagram of the received signal at 6 km range with 10 Gbps data transmission rate.

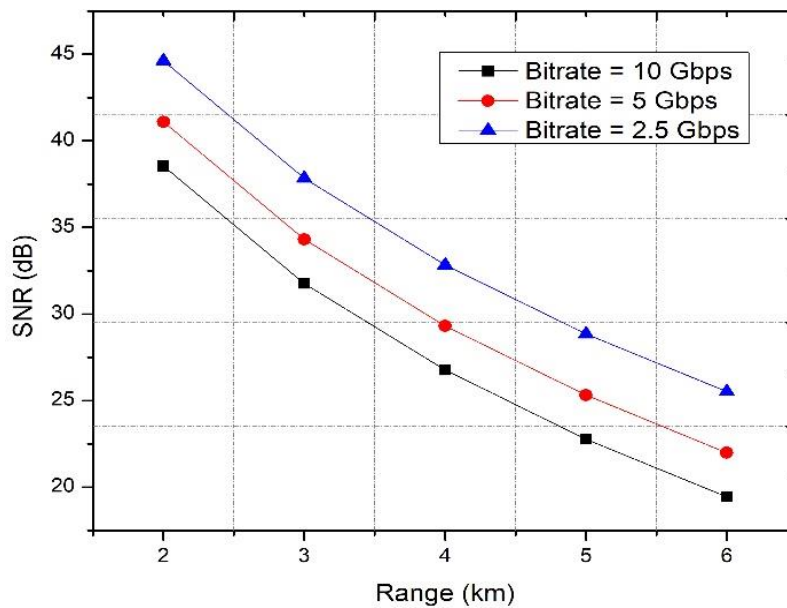


Fig. 4. SNR v/s FSO Range for clear weather (color online)

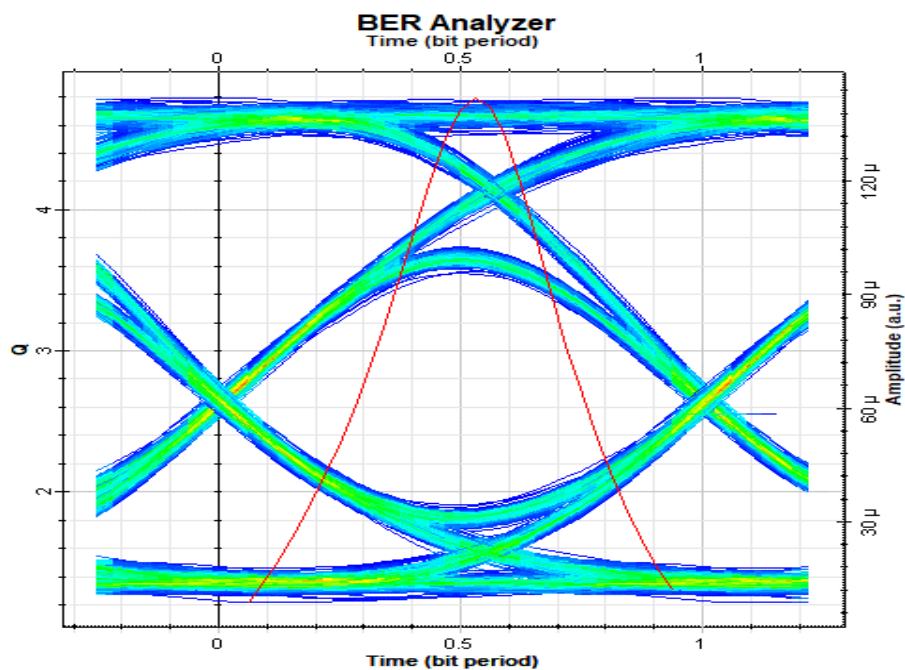


Fig. 5. Eye diagram of the signal at 6 km-10 Gbps for clear weather (color online)

Fig. 6 elucidates the SNR of the received signal for different levels of haze weather with increasing FSO range. Here, the data rate per channel is 10 Gbps and net transmission rate is 320 Gbps. The SNR is 38.97, 27.86, and 19.32 dB at 1500, 2500, and 3500 m respectively for light haze conditions. The SNR is 38.82, 28.88, and 20.34 dB at 1100, 1600, and 2100 m respectively for medium haze conditions. The SNR is 38.52, 27.69, and 17.88 dB at 750, 1050, and 1350 m respectively for heavy haze conditions. Fig. 7(a) – (c) elucidates the eye diagrams of the received signal under haze weather condition.

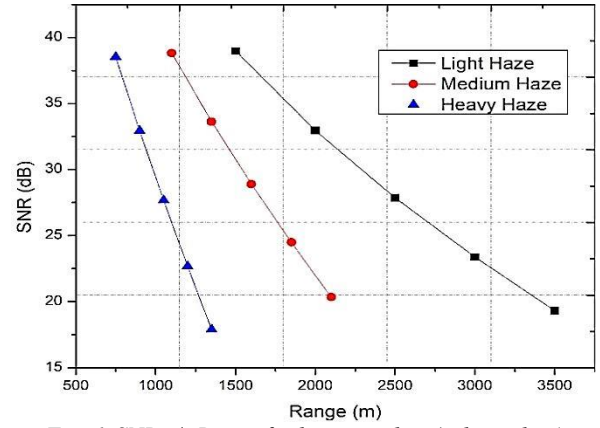


Fig. 6. SNR v/s Range for haze weather (color online)

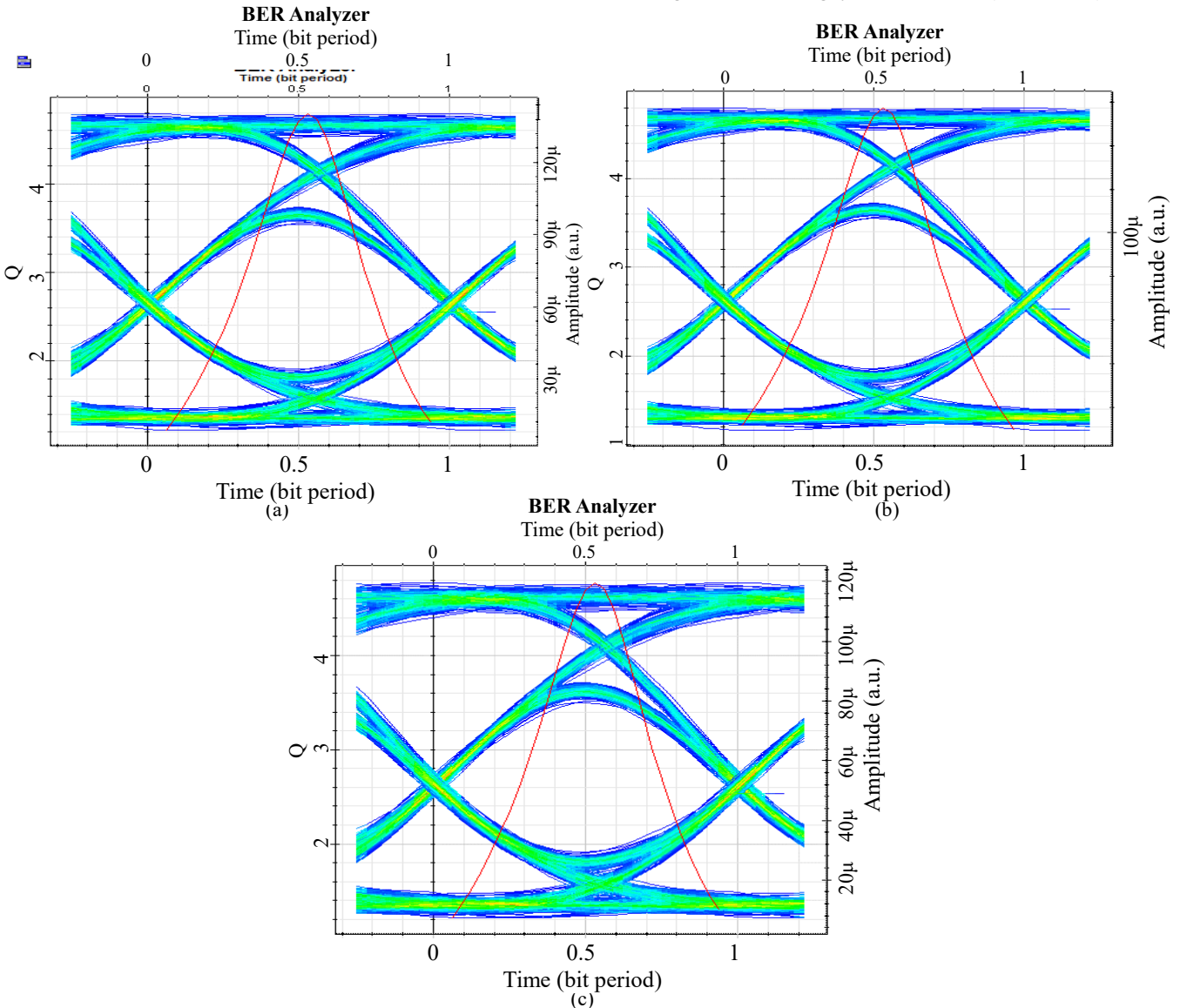


Fig. 7. Eye diagrams of the signal at (a) 3500 m for light haze (b) 2100 m for medium haze (c) 1350 m for heavy haze (color online)

Fig. 8 elucidates the SNR of the received signal for different levels of rain weather with increasing FSO range. The data rate per channel is 10 Gbps and net transmission rate is 320 Gbps. The SNR is 39.86, 28.26, and 18.19 dB at 900, 1350, and 1800 m respectively for light rain conditions. The SNR is 41.14, 30.36, and 20.70 dB at 700,

1000, and 1300 m respectively for medium rain conditions. The SNR is 39.72, 29.97, and 20.84 dB at 500, 660, and 820 m respectively for heavy rain conditions. Fig. 9 (a) – (c) elucidates the eye diagrams of the received signal under haze weather condition.

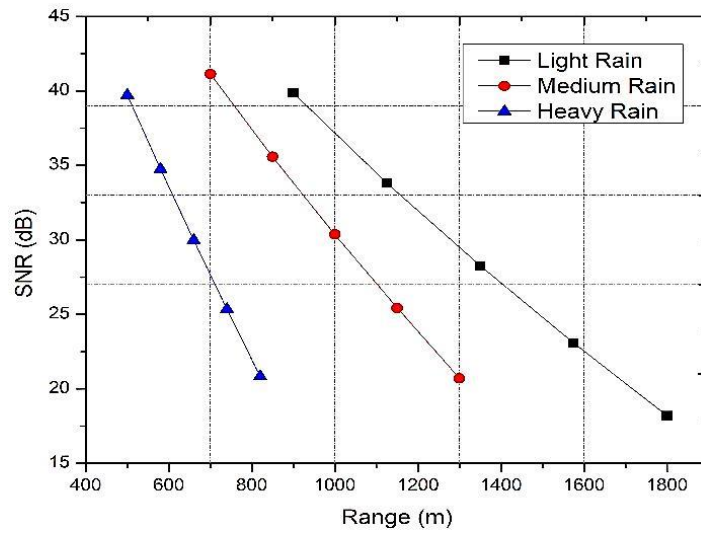


Fig. 8. SNR v/s Range for rain weather (color online)

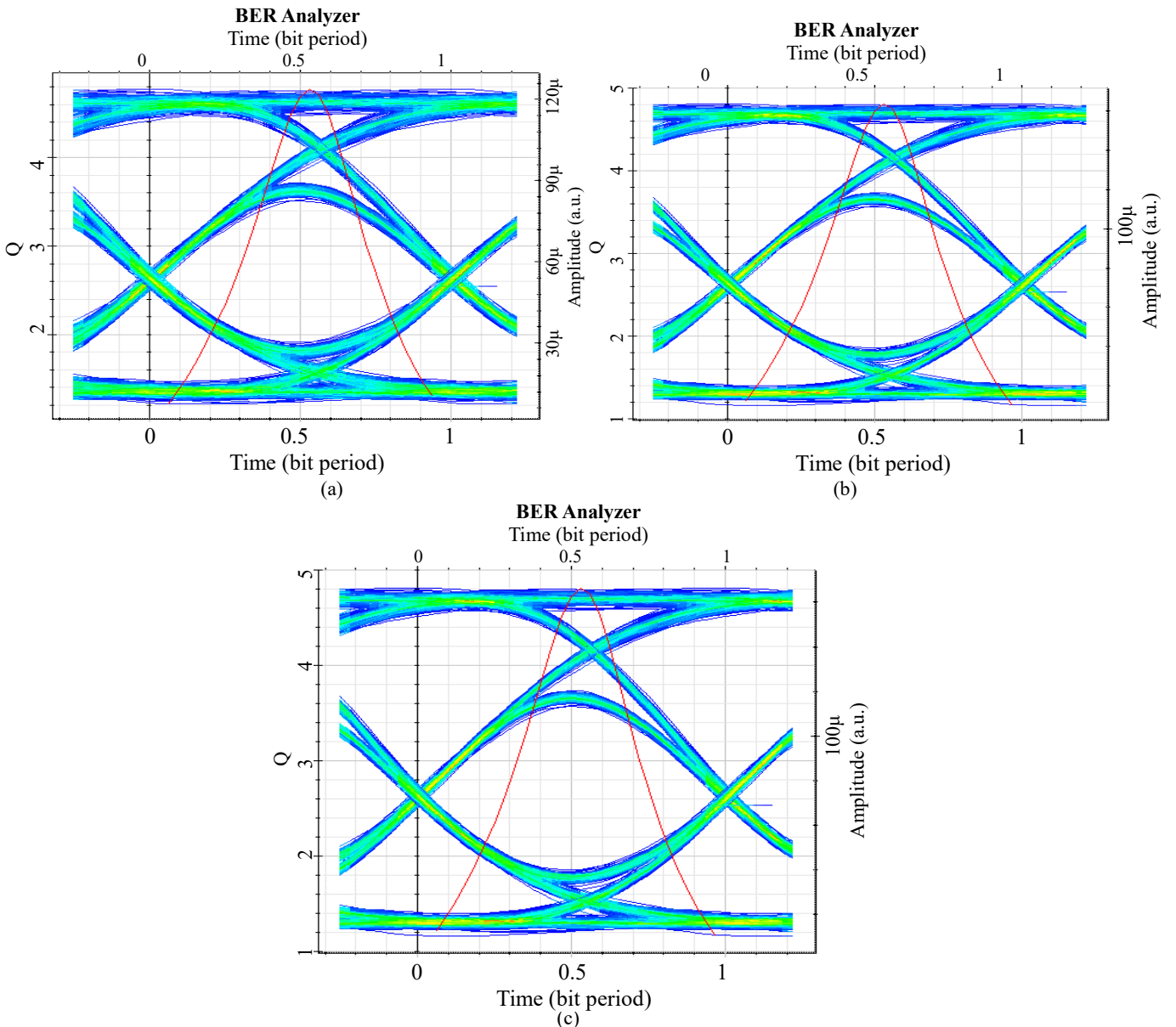


Fig. 9. Eye diagrams of the signal at (a) 1800 m for light rain (b) 1300 m for medium rain (c) 820 m for heavy rain (color online)

Fig. 10 elucidates the SNR of the received signal for different levels of fog weather with increasing FSO range. The data rate per channel is 10 Gbps and net transmission rate is 320 Gbps. The SNR is 38.40, 28.45, and 19.44 dB at 800, 1100, and 1400 m respectively for light fog conditions. The SNR is 37.48, 28.44, and 19.98 dB at 600, 775, and 950 m respectively for medium fog conditions. The SNR is 38.38, 28.32, and 18.83 dB at 480, 630, and 780 m respectively for heavy fog conditions. Fig. 11 (a) – (c) elucidates the eye diagrams of the received signal under haze weather condition.

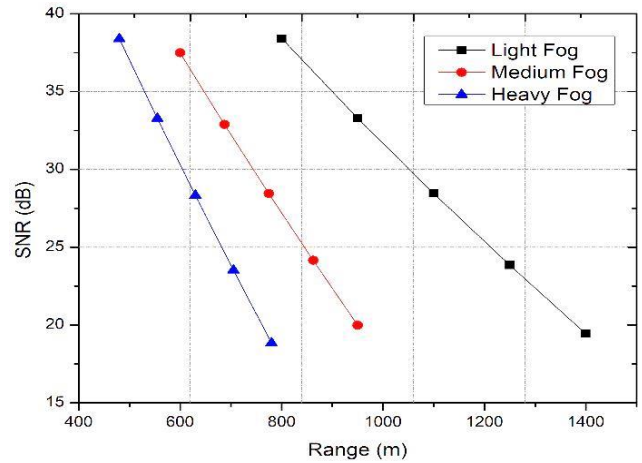


Fig. 10. SNR v/s Range for fog weather (color online)

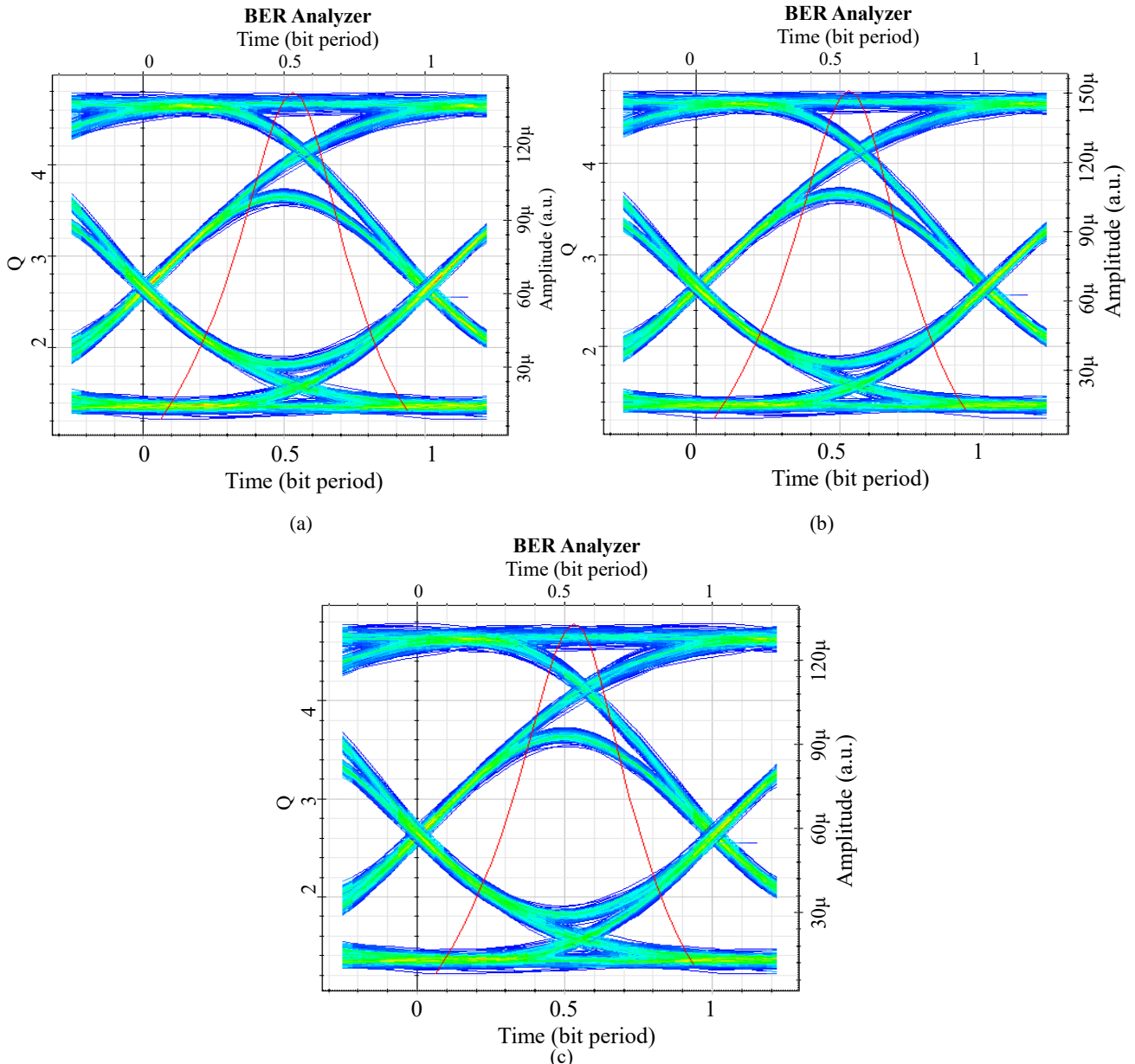


Fig. 11. Eye diagrams of the signal at (a) 1400 m for light fog (b) 950 m for medium fog (c) 780 m for heavy fog (color online)

Table 3 tabulates the maximum achieved link range under different weather conditions with acceptable SNR of the received signals.

Table 3. Maximum achieved link range

Weather	Maximum achieved range
Clear	6 km
Light Fog	1400 m
Light Haze	3500 m
Light Rain	1800 m
Medium Fog	950 m
Medium Haze	2100 m
Medium Rain	1300 m
Heavy Fog	780 m
Heavy Haze	1350 m
Heavy Fog	820 m

4. Conclusions

We have reported a novel high-speed integrated MDM-DWDM-FSO transmission system. 2 spatial LG modes of 16 independent wavelength channels are utilized to carry 10 Gbps data of 32 users to realize a net transmission rate of 320-Gbps. The proposed system is evaluated for different environmental conditions and the achieved range is 6 km for clear; 1400, 3500, and 1800 m for light fog, haze, and rain respectively; 950, 2100, and 1300 m for medium fog, haze, and rain respectively; and 780, 1350, and 820 m for heavy fog, haze, and rain respectively. The proposed system needs to be physically implemented to incorporate the pointing error losses and losses due to real-time environmental effects. In future works, higher order modes such as Hermite-Gaussian and Donut modes will be incorporated in the system to enhance the spectral bandwidth efficiency and data rate of the system. The proposed system can be utilized to meet the high data transmission rates requirement in 5G and beyond 5G networks.

References

- [1] Arun K. Majumdar, *Advanced Free Space Optics (FSO): A Systems Approach*, Springer, New York (2015).
- [2] M. A. Khalighi, M. Uysal, *IEEE Communications Surveys & Tutorials* **16**(4), 2231 (2014).
- [3] Arun K. Majumdar, Jennifer C. Ricklin, *Free-Space Laser Communications: Principles and Advances*, Springer, New York (2008).
- [4] J. Singh, N. Kumar, *Optik* **124**(20), 4651 (2013).
- [5] M. J. Rosker, H. B. Wallace, *Imaging through the atmosphere at terahertz frequencies. Proc. of IEEE/MTT - S International Microwave Symposium, Honolulu, USA*, pp. 773 – 776 (2007).
- [6] A. J. Seeds, H. Shams, M. J. Fice, C. C. Renaud, *Journal of Lightwave Technology* **33**(3), 579 (2015).
- [7] Abhishek Sharma, Kuldeep Singh, Jyoteesh Malhotra, *Journal of Optical Communications* <https://doi.org/10.1515/joc-2023-0295> (2023).
- [8] Abhishek Sharma, Vivekanand Mishra, *Journal of Optical Communications* <https://doi.org/10.1515/joc-2023-0348> (2023).
- [9] K. H. Shakthi Murugan, A. Sharma, J. Malhotra, *Opt. Quant. Electron.* **52**, 505 (2020).
- [10] A. Sharma, J. Malhotra, *Opt. Quant. Electron.* **54**, 233 (2022).
- [11] A. Sharma, J. Malhotra, *Opt. Quant. Electron.* **54**, 410 (2022).
- [12] Abhishek Sharma, Jyoteesh Malhotra, *Journal of Optical Communications* <https://doi.org/10.1515/joc-2023-0176> (2023).
- [13] Hemani Kaushal, Georges Kaddoum, *IEEE Communications Surveys & Tutorials* **19**(1), 57 (2017).
- [14] M. A. Esmail, H. Fathallah, M. Alouini, *IEEE Communications Letters* **20**(9), 1888 (2016).
- [15] H. Singh, N. Mittal, R. Miglani, A. K. Majumdar, **2021** Third South American Colloquium on Visible Light Communications (SACVLC), Toledo, Brazil, p. 01-06 (2021).
- [16] R. Miglani, H. Singh, **2022** International Workshop on Fiber Optics in Access Networks (FOAN), Valencia, Spain, p. 10-15, (2022).
- [17] A. Amphawan, S. Chaudhary, R. Din, M. N. Omar, **2015** IEEE 11th International Colloquium on Signal Processing & Its Applications (CSPA), Kuala Lumpur, Malaysia, p. 145-149 (2015).
- [18] J. Zhang, F. Li, J. Li, Z. Li, **2017** 16th International Conference on Optical Communications and Networks (ICOON), Wuzhen, China, p. 1-3 (2017).
- [19] A. Amphawan, A. Anwar, S. -K. Ong, J. Sutanto, T. -K. Neo, K. Anwar, **2022** 8th Annual International Conference on Network and Information Systems for Computers (ICNISC), Hangzhou, China, p. 527-532 (2022).
- [20] H. Singh, **2023** 10th International Conference on Signal Processing and Integrated Networks (SPIN), Noida, India, p. 154-158 (2023).
- [21] H. Singh, N. Mittal, R. Miglani, A. K. Majumdar, **2021** Third South American Colloquium on Visible Light Communications (SACVLC), Toledo, Brazil, p. 01-06 (2021).
- [22] R. Miglani, H. Singh, **2022** International Workshop on Fiber Optics in Access Networks (FOAN), Valencia, Spain, p. 10-15 (2022).
- [23] J. Zhang, X. Wu, Z. Li, C. Lu, **2022** 27th OptoElectronics and Communications Conference (OECC) and 2022 International Conference on Photonics in Switching and Computing (PSC), Toyama, Japan, p. 1-3 (2022).
- [24] S. A. Abd El-Mottaleb, M. Singh, H. Y. Ahmed, M. Zeghid, K. S. Nisar, *IEEE Photonics Journal* **15**(4), 1 (2023).
- [25] D. Kakati, R. K. Sonkar, **2020** Conference on Lasers

- and Electro-Optics Pacific Rim (CLEO-PR), Sydney, NSW, Australia, p. 1 (2020).
- [26] A. Ghatak, K. Thyagarajan, Cambridge University Press, New York, NY, 1998.
- [27] S. Chaudhary, B. Lin, X. Tang, X. Wei, Z. Zhou, C. Lin, M. Zhang, H. Zhang, *Opt. Quant. Electron.* **50**, 321(2018).
- [28] S. Chaudhary, L. Wuttisittikulkij, J. Nebhen, X. Tang, M. Saadi, S. Al Otaibi, A. Althobaiti, A. Sharma, S. Choudhary, *Front. Phys.* **9**, 756232 (2021).
- [29] Yogesh Kumar Gupta, Aditya Goel, *Heliyon* **9**, e13325 (2023).

*Corresponding author: amitgrover321@gmail.com